Investigating Anharmonic XAFS Debye-Waller Factor of Crystalline Tungsten Based on Einstein Model

Nguyen Thi Minh Thuy

Faculty of Fundamental Sciences, University of Fire Prevention and Fighting, Hanoi 120602, Vietnam

ABSTRACT: The anharmonic X-ray absorption fine structure (XAFS) Debye-Waller (DW) factor of the crystalline tungsten (W) has been investigated in the temperature-dependent. This DW factor is calculated in explicit forms using the quantum anharmonic correlated Einstein model developed from the correlated Einstein model based on the anharmonic effective potential and the quantum statistical theory. The numerical results of W in the temperature range from 0 to 900 K are in good agreement with those obtained by the other theoretical models and experiments at several temperatures. The analytical results show that the anharmonic correlated Einstein model is suitable for analyzing the experimental XAFS data of metals.

KEYWORDS: XAFS DW factor, thermal disorders, crystalline tungsten, Einstein model

I. INTRODUCTION

In recent years, the X-ray absorption fine structure (XAFS) has been widely used to determine many thermodynamic properties and structural parameters of materials, so it has been developed into a powerful technique [1-2]. However, thermal vibrations cause a change in the atomic positions and their interatomic distances [3-4]. The *K*-edge XAFS oscillation includes a non-Gaussian disorder for a given scattering path is expressed in terms of a canonical average of all distance-dependent factors by [5]

$$\chi(k,T) = \frac{Ne^{-2k^2\sigma^2(T)}f(k)}{kR^2(T)}\sin\left[2kR(T)+\delta(k)\right], \qquad (1)$$

where *T* is the absolute temperature, k is the wave number of the photoelectron, $f(k)$ and $\delta(k)$ characterizes scattering parameters of the photoelectron, $\sigma^2(T)$ describes the thermal disorder in the neighbor distance, $R(T)$ is the distance to the neighboring atom, and N is the number of neighboring atoms.

In the investigation of the anharmonic XAFS signal, the anharmonic XAFS Debye-Waller (DW) factor $\mathrm{W}(T,k)$ [6] is an important parameter. It is because they can describe the anharmonic XAFS amplitude reduction and are determined as follows [7]:

$$\mathrm{W}(T,k) = \exp\left\{-2k^2\sigma^2(T)\right\}, \qquad (2)$$

where σ^2 is the mean-square relative displacement (MSRD) and is the second XAFS cumulant.

Nowadays, crystalline tungsten (W) is a rare metal with a body-centered cubic (BCC) structure. It has also become one of the most important functional materials in modern industry and national defense [8]. For BCC metals, the second XAFS cumulants have also been investigated using the anharmonic correlated Debye (ACD) [11] and classical anharmonic correlated Einstein (CACE) model [12]. However, the obtained expression using the ACD is not explicit and needs many computational steps, and the obtained expression using the CACE is not valid at the low-temperature (LT) region. Meanwhile, the experiment measured the second XAFS cumulants of W at 293 K, 323 K, 373 K, 423 K, 473 K, 523 K, and 573 K were measured the MSRD of W at the Synchrotron Radiation Siberian Center (SRSC), Russia, by Pirog *et al.* [4].

Recently, a quantum anharmonic correlated Einstein (QACE) model has been applied to to effectively treat the anharmonic XAFS oscillation of materials [13-15]. This model has the advantage that the obtained expressions are explicit and valid even in

Investigating Anharmonic XAFS Debye-Waller Factor of Crystalline Tungsten Based on Einstein Model

the LT region. Hence, the analysis and calculation of the anharmonic XAFS DW factor of W using the QACE model will be a necessary addition to the experimental XAFS analysis technique.

II. FORMALISM AND CALCULATION MODEL

Usually, an anharmonic effective (AE) potential can specify the thermodynamic parameters of crystals [16]. This potential can be determined from the pair interaction (PI) potential of atoms. The AE potential can be calculated from the PI potential [17]:

$$V_{eff} = \varphi(x) + \sum_{i=A,B} \sum_{j \neq A,B} \varphi\left(\varepsilon_i x \hat{R}_{AB} \hat{R}_{ij}\right), \ \varepsilon_i = \frac{\mu}{M_i}, \ x = r - r_0, \tag{3}$$

where $\mu = M_A M_B / (M_A + M_B)$ is the reduced mass of the backscatter with masse M_A and absorber with masse M_B, sum i is the over backscatter ($i = A$) and absorber ($i = B$), the sum j is over the nearest neighbors, $\hat{R}$ is a unit vector, and $\varphi(x)$ is a PI potential of these atoms with r and r_0 are the instantaneous and equilibrium bond length between atoms, respectively.

Figure 1. The structural model of W.

The structural model of W is illustrated in Fig. 1, which has similar atoms at one center and eight corners of a cube [18], so each atom has a mass of m, and each unit cell contains two atoms [19]. The AE potential of W is calculated from Eq. (3) and is written as

$$V_{eff}(x) = \varphi(x) + \varphi(0) + 2\varphi\left(-\frac{1}{2}x\right) + 6\varphi\left(-\frac{1}{6}x\right) + 6\varphi\left(\frac{1}{6}x\right), \tag{4}$$

For metal crystals, the Morse potential can validly describe the PI potential [20]. It is presented by expanding this potential to the third order around its minimum position as

$$\varphi(x) = D\left(e^{-2\alpha x} - 2e^{-\alpha x}\right) \cong -D + D\alpha^2 x^2 - D\alpha^3 x^3, \tag{5}$$

where α is the dissociation energy, D is the width of the potential,

The result of AE potential can be obtained from Eq. (4) using Morse potential in Eq. (5). If ignoring the overall constant, it is presented in the form:

$$V_{eff}(x) = \frac{1}{2}k_0 x^2 - k_3 x^3, \tag{6}$$

where k_{eff} is the effective force constant, and k_{an} is an anharmonic force constant [21], which are not temperature-dependent and are written as

$$k_{eff} = \frac{11}{3}D\alpha^2, \quad k_{an} = \frac{3}{4}D\alpha^3, \tag{7}$$

The QACE model [13] was developed from the CE model [22] based on the first-order perturbation (FOP) theory [21] and AE potential [17]. In this model, the atomic thermal vibrations in the crystal lattice of W can be characterized by the correlated Einstein temperature θ_E and frequency ω_E [15]. These parameters can be defined as follows:

$$\omega_E = \sqrt{\frac{k_{eff}}{\mu}} = \alpha\sqrt{\frac{22D}{3m}}, \quad \theta_E = \frac{\hbar\omega_E}{k_B} = \frac{\hbar\alpha}{k_B}\sqrt{\frac{22D}{3m}}, \tag{8}$$

where $\hbar$ and k_B are the reduced Planck and Boltzmann constants, respectively.

Investigating Anharmonic XAFS Debye-Waller Factor of Crystalline Tungsten Based on Einstein Model

Usually, the second XAFS cumulants can be presented in terms of the power moments $\langle x^k \rangle$ with $\langle \ \rangle$ is the thermal average and are approximated via the statistical density matrix within the quantum-statistical theory. The general expressions of the temperature-dependent XAFS cumulants in the QACE model were calculated by Tien *et al.* [13]. Substituting the expressions of local force constants k_{eff} and k_{an} in Eq. (7) into the general expression of the second XAFS cumulant, we obtain the temperature-dependent second XAFS cumulant in the form as

$$\sigma^2(T) = \left\langle (r-R)^2 \right\rangle = \left\langle x^2 \right\rangle - \left\langle x \right\rangle^2 = \frac{3\hbar\omega_E}{22D\alpha^2}\left(\frac{e^{\hbar\omega_E/k_B T}+1}{e^{\hbar\omega_E/k_B T}-1}\right), \qquad (9)$$

Substituting this cumulants into the Eq. (2) to calculate the temperature-dependent XAFS DW factor of W, we obtain the following result:

$$\mathrm{W}(T,k) = \exp\left\{-\frac{3\hbar\omega_E}{11D\alpha^2}\left(\frac{e^{\hbar\omega_E/k_B T}+1}{e^{\hbar\omega_E/k_B T}-1}\right)k^2\right\}, \qquad (10)$$

Thus, the QACE model has been extended to calculate the temperature-dependent XAFS DF factor of W efficiently. The expressions obtained using this model can satisfy all their fundamental properties in temperature dependence.

III. RESULTS AND DISCUSSION

In this section, the numerical results of W are calculated using the QACE model based on the obtained expressions in Secs. 2 and their physical parameters, which are the atomic mass $m = 183.85$ u [23] and Morse potential parameters $D = 0.9906$ eV, $\alpha = 1.4116$ Å^{-1}, and $r_0 = 3.032$ Å [24]. We calculate using Eqs. (7) and (8) in the QACE model and obtain the local force constants $k_{eff} \ \square \ 7.24$ eVÅ^{-2}, $k_{an} \ \square \ 2.09$ eVÅ^{-3}, the correlated Einstein frequency $\omega_E \ \square \ 2.75 \times 10^{13}$ Hz, and the correlated Einstein temperature $\theta_E \ \square \ 209.92$ K. Meanwhile, the respective values obtained from the experiment are $k_{eff} \ \square \ 9.0 \pm 0.9$ eVÅ^{-2}, $k_{an} \ \square \ 3.5 \pm 0.8$ eVÅ^{-3}, $\omega_E \ \square \ 2.8 \pm 0.2 \times 10^{13}$ Hz, and $\theta_E \ \square \ 214.0 \pm 12.0$ K [4]. Our results do not differ much from the experimental values, especially regarding the correlated Einstein frequency and temperature.
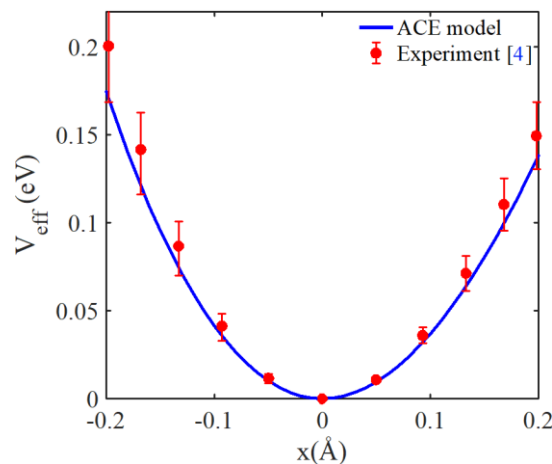
Figure 2. The position-dependent AE potential of W is obtained from the QACE and experiment.

The position dependence of the AE potential of W in the position range from - 0.2 to 0.2 Å is represented in Fig. 2. Our obtained result using the QACE model is calculated by Eqs. (6) and (7), while the experimental result is obtained from Eq. (6) with the experimental values of local force constants $k_{eff} \ \square \ 9.0 \pm 0.9$ eVÅ^{-2} and $k_{an} \ \square \ 3.5 \pm 0.8$ eVÅ^{-3} [4]. Our result agrees better with those obtained from the experiment [4], especially at positions far from the minimum position. Moreover, the influence of anharmonic effects on the AE potential is stronger at positions further away from the minimum position of this potential.

Investigating Anharmonic XAFS Debye-Waller Factor of Crystalline Tungsten Based on Einstein Model
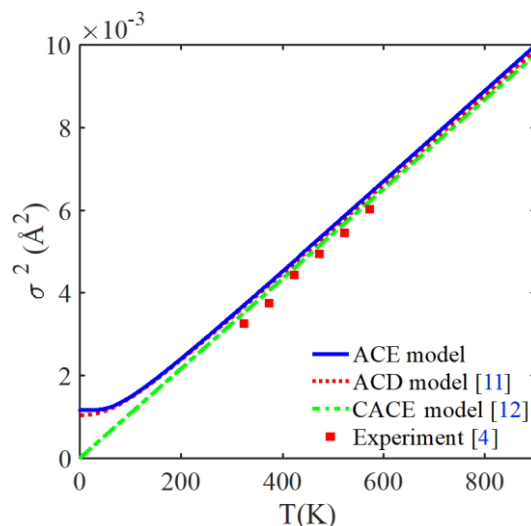
Figure 3. Temperature-dependent second cumulants of W is obtained using the QACE, ACD, and CACE models and experiment.

The temperature dependence of the second XAFS cumulant $\sigma^2(T)$ of W in a range from 0 K to 900 K is represented in Fig. 3. Our obtained result using the QACE model is calculated by Eq. (9). It can be seen that our results are in agreement with those obtained using the ACD [11] and CACE (only at the high temperatures) [12] models and experiment [4]. For example, the obtained results using the QACE model, ACD model, CACE model, and experiment at $T = 423$ K are $\sigma^2 \square\ 4.76\times10^{-3}$ Å², $\sigma^2 \square\ 4.69\times10^{-3}$ Å² [11], $\sigma^2 \square\ 4.64\times10^{-3}$ Å² [12], and $\sigma^2 \square\ 4.34\times10^{-3}$ Å² [4], respectively. Moreover, it can be seen that the QACE and ACD [11] models both show quantum effect contributions, but the obtained results using the QACE model in the LT region are slightly greater. Meanwhile, the obtained results using the CACE model [12] approach zero as the temperature approaches zero, so this model can not work well in the LT region.
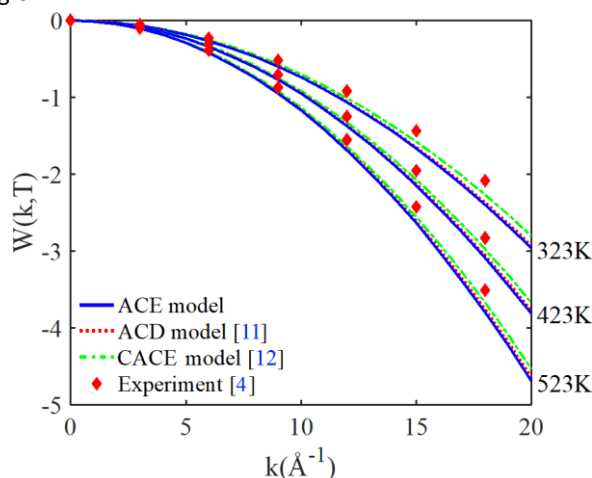
Figure 4. The influence of temperature change on the wavenumber-dependent XAFS DW factor of W is obtained using the QACE, ACD, and CACE models and experiment.

The wavenumber dependence of the anharmonic XAFS DW factor of W at 323 K, 423 K, and 523 K and in a range from 0 to 20 Å is represented in Fig. 4. Herein, the obtained results using the ACD and CACE model are calculated by Eq. (2), with the temperature-dependent second XAFS cumulant determined in Refs. 11 and 12, respectively. Our obtained results using the QACE model are calculated by Eq. (10), while the obtained results using the experiment are calculated by Eq. (2) with the experimental values of the second XAFS cumulant in Ref. 4. It can be seen that our results agree with those obtained using the ACD [11] and CACE [12] models and experiment [4], especially in comparison with the obtained results using the ACD model. Moreover, the values of the XAFS DW factor decrease with increasing temperature *T* and decrease with fast-increasing wavenumber *k*. It is because the XAFS DW factor is an inverse function of the wavenumber *k* and second XAFS cumulant, in which this cumulant increases with increasing temperature *T,* as seen in Eq. (2) and Fig. 3.

Investigating Anharmonic XAFS Debye-Waller Factor of Crystalline Tungsten Based on Einstein Model

Thus, the calculated results of the anharmonic XAFS DW factor using the present QACE model satisfied all of their fundamental properties. The anharmonic XAFS DW factor decreases with increasing temperature T. It means that the XAFS amplitude decreases more strongly at higher temperatures. These results can also describe the influence of anharmonic effects at high temperatures and the influence of quantum effects at low temperatures.

IV. CONCLUSION

In this investigation, we have expanded and developed an efficient model to calculate and analyze the anharmonic XAFS DW factor of W. The anharmonic XAFS DW factor decreases with increasing temperature T. It means that anharmonic XAFS amplitude decreases more strongly at higher temperatures. These results can also describe the influence of anharmonic effects at high temperatures and the influence of quantum effects at low temperatures on the XAFS oscillation. The agreement between our numerical results of W and those obtained using the ACD and CACE models and experiments at various temperatures shows the effectiveness of the present model in investigating the anharmonic XAFS DW factor. This model can be applied to calculate and analyze the anharmonic XAFS DW factor of other metals from above absolute zero temperature to just before the melting point.

REFERENCES

1. P. Fornasini, R. Grisenti, M. Dapiaggi, G. Agostini, and T. Miyanaga, "Nearest-neighbour distribution of distances in crystals from extended X-ray absorption fine structure," Journal of Chemical Physics, Vol. 147, No. 4, pp. 044503, 2017.
2. P. A. Lee, P. H. Citrin, P. Eisenberger, and B. M. Kincaid, "Extended x-ray absorption fine structure its strengths and limitations as a structural tool," Reviews of Modern Physics, Vol. 53, No. 4, pp. 769-806, 1981.
3. P. Eisenberger and G. S. Brown, "The study of disordered systems by EXAFS: Limitations," Solid State Communications, Vol. 29, No. 6, pp. 481-484, 1979.
4. I.V. Pirog and T.I. Nedoseikina, "Study of effective pair potentials in cubic metals," Physica B: Condensed Matter, Vol. 334, No. 2, pp. 123-129, 2003.
5. M. Newville, "Fundamentals of XAFS," Reviews in Mineralogy & Geochemistry, Vol. 78, No. 1, pp. 33-74, 2014.
6. R. B. Greegor and F. W. Lytle, "Extended x-ray absorption fine structure determination of thermal disorder in Cu: Comparison of theory and experiment," Physical Review B, Vol. 20, No. 12, pp. 4902-4907, 1979.
7. N. V. Hung, C. S. Thang, N. B. Duc, D. Q. Vuong, and T. S. Tien, "Temperature dependence of theoretical and experimental Debye-Waller factors, thermal expansion and XAFS of metallic Zinc," Physica B: Condensed Matter, Vol. 521, pp. 198-203, 2017.
8. E. Lassner, W. D. Schubert, E. Lüderitz, and H. U. Wolf, Tungsten, Tungsten Alloys, and Tungsten Compounds, Weinheim: Wiley-VCH, 2000.
9. K. Turrell, Tungsten (Elements), New York: Benchmark Books, 2004.
10. John Emsley, Nature's Building Blocks: An AZ Guide to the Elements, 2nd ed. New York: Oxford University Press, 2011.
11. N. V. Hung, T. T. Hue, H. D. Khoa, and D. Q. Vuong, "Anharmonic correlated Debye model high-order expanded interatomic effective potential and Debye-Waller factors of bcc crystals," Physica B: Condensed Matter, Vol. 503, pp. 174-178, 2016.
12. T.S. Tien, "Temperature dependence of EXAFS spectra of BCC crystals analyzed based on classical anharmonic correlated Einstein model," Journal of Theoretical and Applied Physics, Vol. 14, No. 3, pp. 295-305, 2020.
13. T.S. Tien, "Advances in studies of the temperature dependence of the EXAFS amplitude and phase of FCC crystals," Journal of Physics D: Applied Physics, Vol. 53, No. 11, pp. 315303, 2020.
14. T.S. Tien, "Investigation of the anharmonic EXAFS oscillation of distorted HCP crystals based on extending quantum anharmonic correlated Einstein model," Japanese Journal of Applied Physics, Vol. 60, No. 11, pp. 112001, 2021.
15. T. S. Tien, N. V. Nghia, C. S. Thang, N. C. Toan, and N. B. Trung, "Analysis of temperature-dependent EXAFS Debye-Waller factor of semiconductors with diamond crystal structure," Solid State Communications, Vol. 352, pp. 114842, 2022.
16. N. V. Hung, L. H. Hung, T. S. Tien, and R. R. Frahm, "Anharmonic effective potential, effective local force constant and EXAFS of hcp crystals: Theory and comparison to experiment," International Journal of Modern Physics B, Vol. 22, No. 29, pp. 5155-5166, 2008.
17. N. V. Hung and J. J. Rehr, "Anharmonic correlated Einstein-model Debye-Waller factors," Physical Review B, Vol. 56, No. 1,

pp. 43-46, 1997.

18. S. H. Simon, The Oxford Solid State Basics, 1st ed. Oxford: Oxford University Press, 2013.

19. I. L. Shabalin, Ultra-High Temperature Materials I, New York: Springer, 2014.

20. P. M. Morse, "Diatomic Molecules According to the Wave Mechanics. II. Vibrational Levels," Physical Review, Vol. 34, pp. 57-64, 1929.

21. T. Yokoyama, K. Kobayashi, T. Ohta, and A. Ugawa, "Anharmonic interatomic potentials of diatomic and linear triatomic molecules studied by extended x-ray-absorption fine structure," Physical Review B, Vol. 53, No. 10, pp. 6111-6122, 1996.

22. E. Sevillano, H. Meuth, and J. J. Rehr, "Extended x-ray absorption fine structure Debye-Wailer factors. I. Monatomic crystals," Physical Review B, Vol. 20, No. 12, pp. 4908-4911, 1979.

23. N. W. Ashcroft and N. D. Mermin, Solid State Physics, 1st ed. New York: Holt-Rinehart & Winston, 1976.

24. L. A. Girifalco and V. G. Weizer, "Application of the Morse Potential Function to Cubic Metals," Physical Review, Vol. 114, No. 3, pp. 687-690, 1959.